

Current-Driven Magnetization Dynamics in Magnetic Multilayers

S. Urazhdin

*Department of Physics and Astronomy, Center for Fundamental Materials Research and Center for Sensor Materials,
Michigan State University, East Lansing, MI 48824*

(Dated: November 19, 2018)

We show that spin-polarized current flowing through a ferromagnet leads to predominantly incoherent magnetic excitations. We describe these excitations by an effective magnetic temperature rather than a coherent precession as in the popular spin-torque model. Our model reproduces all the essential features of the experiments, and gives several predictions that distinguish it from the spin-torque model.

I. INTRODUCTION

Electrons injected into a ferromagnet lead to excitation or reversal of magnetization. This effect was predicted by Slonczweski¹ and Berger,² and later observed experimentally.^{3,4} Most of the magnetization switching experiments are performed with trilayers of structure $F_1/N/F_2$, where a thick and usually extended ferromagnet F_1 plays a role of electron current polarizer not affected by the current, N is a nonmagnetic spacer separating the magnetic layers, and F_2 is nanopatterned into a typically elongated nanopillar of submicrometer dimensions. The current-driven magnetization switching of the nanopillar F_2 usually occurs between two well-defined orientations along the magnetic easy axis defined by the nanopillar shape anisotropy. This is the specific experimental situation we will be dealing with in this paper.

Both of the original models^{1,2} in different ways rely on transfer of spin from the polarized electron current to the ferromagnet. Berger considered generation of magnons by spin-flipping of electrons, driven by the spin accumulation. Slonczewski considered the electron spin component transverse to the magnetization, which is absorbed by the ferromagnet due to a combination of spin-dependent reflection at the interfaces and averaging of the electron spin precession phases in the ferromagnet. The resulting torque drives the magnetic dynamics. In another model, proposed later by Heide *et al.*,⁵ the effect of current was described as a nonequilibrium exchange interaction between F_1 and F_2 . This interaction was similar to an effective current-dependent field. Later experimental results were found to be inconsistent with this effective field model.^{6,7,8}

The spin-torque model (ST) has become dominant in the interpretation of experiments.^{3,6,7,8,15,16,17,18,19,20,21} A few exceptions include some of the point contact measurements, interpreted in terms of resonant electron-magnon scattering,^{4,9} and thermally activated switching, interpreted in terms of incoherent current-driven excitations, described as an effective magnetic temperature.^{10,11,12,13} With various extensions and modifications, incorporating incomplete current polarization, band structure, spin accumulation, thermal activation, and inhomogeneous magnetization states, ST is also dominant in theoretical re-

search.^{17,22,23,24,25,26,27,28,29,30,31,32,33}

Despite the overall success of ST, several fundamental issues remain unresolved. First, approximation of the magnetization by a classical macrospin is essential for the coherent dynamics predicted by the model. On the other hand, finite-wavelength magnetic excitations (magnons) are also found to be excited in certain extensions of ST, thus violating the assumptions underlying the model.³⁴ A large number of the excited magnetic modes then need to be considered to adequately describe the current-driven magnetic dynamics. This situation is fundamentally different from the magnetic excitation by ac field in transverse ferromagnetic resonance (FMR) experiments, where only uniform precession is excited by the ac magnetic field, because nonuniform excitations do not couple to this field. On a more fundamental level, the relation of ST to the quantum-mechanical picture involving electron-magnon scattering is not understood. Among related issues, energy transfer from the current to the magnetic system, and the magnetic dynamics induced by scattering of a single electron, are not addressed by the classical ST.

The first goal of this paper is to critically examine the fundamentals of ST, and its relation to the quantum-mechanical electron-magnon scattering picture. In Section II, we consider a toy-model quantum analog of ST, i.e. a model involving the quantum dynamics of both the nanopillar magnetization, treated as a macrospin, and current-carrying electrons. In addition to the ST result for the coherent magnetic excitations, this model gives incoherent (i.e. not described as a classical precession) excitations. In the typical experiments, where the polarization of the current is initially e.g. antiparallel to the magnetization, the coherent excitation vanishes, while the incoherent excitation rate is largest. Current-driven generation of finite-wavelength magnons, and magnon interactions further decrease the coherence of the excitation. In Section III, we use a ballistic scattering approach, where the magnetic excitations are approximately described as increase of a magnetic temperature, to obtain the magnetization switching in nanopillars. Our model reproduces all of the experimental current-switching behaviors, and gives several predictions that distinguish it from ST.

II. TWO-SPIN SCATTERING MODEL

In this section, we solve a simple model for the interaction of a conduction electron with a ferromagnet F_2 , and show how the result relates both to ST¹ and electromagnon scattering framework.² We model F_2 by a large spin in the state $|\mathbf{S}\rangle = |L, M\rangle \equiv |M\rangle$, where L is fixed, and M is its projection on the quantization axis z , aligned with the effective magnetic field H_{eff} . H_{eff} includes both the applied field and the anisotropy field of the nanopillar. We define the exchange stiffness of a ferromagnet as the exchange contribution to the dispersion of the spin-waves in the bulk of the ferromagnet. In typical experiments, the ratio of the exchange stiffness of F_2 to its largest dimension is significantly smaller than the typical energies of conduction electrons scattered by this layer (measured from the Fermi level). Thus, finite-wavelength magnetic modes are expected to be excited by the current, which cannot be described in the fixed- L (macrospin) approximation. When we relate our results to experiments in Section III, the macrospin approximation is not used. In the present Section, we use the macrospin approximation both for comparison to ST, which makes a similar approximation, and due to the transparency of the results.

We assume that F_2 is a transition metal. The magnetic properties of transition metals are dominated by the $3d$ electrons, while transport occurs through the more mobile states of predominantly $4s$ type. The hybridization between the conduction electrons and the magnetization is approximately described by a Stoner exchange potential $V_{\text{ex}} = (J/L)\mathbf{S} \cdot \mathbf{s}$, where s is the conduction electron spin. The pre-factor (J/L) explicitly accounts for the independence of the exchange potential of the size of the ferromagnet. If the orbital part of the electron wave function is included, V_{ex} gives spin-dependent reflection at the magnetic interfaces. We omit the orbital part, concentrating on the spin dynamics.

H_{eff} can be ignored when solving the problem of scattering of the conduction electrons by F_2 , since the associated Zeeman energy is typically five orders of magnitude smaller than V_{ex} . When an electron is far from the ferromagnet before scattering, it is in the state $|\mathbf{s}\rangle = |\alpha| \uparrow\rangle + |\beta| \downarrow\rangle$. To solve the scattering problem, we express the electron wavefunction through the angular momentum eigenstates

$$\begin{aligned} \sqrt{2L+1}\psi_i = & \sqrt{2L+1}(|\alpha| \uparrow\rangle + |\beta| \downarrow\rangle) |L, M\rangle = \\ & \alpha\sqrt{L+M+1} |L+1/2; M+1/2\rangle + \\ & \beta\sqrt{L-M+1} |L+1/2; M-1/2\rangle - \quad (1) \\ & \alpha\sqrt{L-M} |L-1/2; M+1/2\rangle + \\ & \beta\sqrt{L+M} |L-1/2; M-1/2\rangle . \end{aligned}$$

Here $|j; j_z\rangle$ denote the states with total spin j and z -projection j_z . $V_{\text{ex}} = J$ for the first two terms on the right, and $V_{\text{ex}} = -J\frac{L-1}{L} \approx -J$ for the last two terms. We turn on the interaction for the time an electron at the Fermi

energy spends in F_2 , $t \approx 10^{-15}$ sec for a several nm thick magnetic layer. In transition metal ferromagnets, $V_{\text{ex}} \approx -1$ eV gives a similar time scale for the spin dynamics, $V_{\text{ex}}/\hbar \approx 1-10 \times 10^{-15}$ sec. Scattering gives a phase shift $\phi \approx 10^0 - 10^1$ between the $j = L-1/2$ and $j = L+1/2$ terms in Eq. 1. The final state in the basis of individual spins is

$$\begin{aligned} (2L+1)\psi_f = & \\ \alpha|\uparrow\rangle |M\rangle & [L+M+1 + e^{i\phi}(L-M)] + \\ \alpha|\downarrow\rangle |M+1\rangle & \sqrt{(L-M)(L+M+1)}(1-e^{i\phi}) + \quad (2) \\ \beta|\downarrow\rangle |M\rangle & [L-M+1 + e^{i\phi}(L+M)] + \\ \beta|\uparrow\rangle |M-1\rangle & \sqrt{(L+M)(L-M+1)}(1-e^{i\phi}). \end{aligned}$$

To compare with ST, we first consider $L = M$, an example of a coherent state of F_2 . We calculate the electron spin components. Since V_{ex} conserves the total spin, identical results are obtained with similar calculations for \mathbf{S} . Take α, β real, then only x - and z -components of the electron spin before scattering are finite

$$\langle \psi_i | s_x | \psi_i \rangle = \alpha\beta, \langle \psi_i | s_z | \psi_i \rangle = (\alpha^2 - \beta^2)/2. \quad (3)$$

For the final state (Eq. 2), we first find expectation values of spin components, and then average over ϕ due to its strong variation with t for different electron paths in F_2 . Analysis involving an actual integration over the different paths is expected to yield similar results.^{28,30}

$$\begin{aligned} \langle \psi_f | s_y | \psi_f \rangle_{av} &= 0, \langle \psi_f | s_x | \psi_f \rangle_{av} = \alpha\beta/(2L+1) \\ \langle \psi_f | s_z | \psi_f \rangle_{av} &= (\alpha^2 - \beta^2[1 - \frac{8L}{(2L+1)^2}])/2. \quad (4) \end{aligned}$$

To avoid confusion, we note that ST considers the reference frame set by the orientation of \mathbf{S} . This frame coincides with our x, y, z frame only in the special case $M = L$. The x - and z -components of electron spin are then usually referred to as longitudinal and transverse spin components, respectively, as defined with respect to the orientation of \mathbf{S} . For large L , Eq. 4 shows that all the transverse electron spin is absorbed by \mathbf{S} , while the change of the longitudinal spin is small, $\Delta s_z \propto 1/L$. If $H_{\text{eff}} = 0$, \mathbf{S} subsequently relaxes to a classical state with a new direction determined by the spin conservation $\sin(\theta) \approx \Delta s_z/L$, or $\theta \approx \frac{\alpha\beta}{L}$. Here θ is the angle between the new orientation of \mathbf{S} and the z -axis. A similar conclusion is reached by ST.¹

A different result is expected at finite H_{eff} along the z -axis. For the sake of argument, assume that scattering of electrons classically tilts \mathbf{S} away from its equilibrium orientation along H_{eff} . \mathbf{S} subsequently starts precessing around H_{eff} , relaxing back to its equilibrium state. It is well established in the ferromagnetic resonance (FMR) experiments, that the magnetic relaxation can be separated into two channels, characterized by the relaxation rates T_1 and T_2 .³⁵

T_1 characterizes the relaxation of the total magnetic energy, mostly due to scattering with the conduction electrons and phonons. In current-driven switching experiments, the magnetic energy relaxation into conduction

electrons is partly blocked by the same mechanism that gives rise to the current-driven excitation. Thus, T_1 is expected to be larger than in the FMR experiments with films of the same thickness as F_2 . The magnetic energy relaxation is measured as a variation of $n = L - M$, which we call the number of magnons. This definition needs to be expanded when including nonuniform magnetic excitations, which reduce the length of \mathbf{S} . We do not perform the Holstein-Primakoff transformation, so the magnons only approximately obey Bose-Einstein statistics at $n \ll L$.³⁶

T_2 characterizes the relaxation of the uniform precession, which, in addition to the processes contributing to T_1 , also includes scattering of the uniform precession into other magnetic modes, through nonlinear magnetic interactions. Generally, $T_2 < T_1$.³⁵ In current-switching experiments, the nonlinear magnetic interactions are enhanced (compared to the values for small amplitude FMR in bulk ferromagnets) by high excitation levels associated with the switching,³⁷ and by scattering at the surfaces of the thin layer F_2 .^{35,38}

The relation $T_2 < T_1$ allows for nonequilibrium populations of all the magnetic modes, even if only the uniform precession is excited by the current. Moreover, we argue below that the current-driven excitations themselves (regardless of the T_2 processes) are at least partly incoherent, and many finite-wavelength modes are directly excited by the current. Thus, we expect that at sufficiently long excitation times (e.g. when a dc current is applied), the uniform precession is only a small part of the generally incoherent steady magnetization state. General arguments of statistical physics tell us that the nonlinear magnetic interactions tend to thermalize the magnetic excitations. In Section III, the excited state is approximately described by an effective magnetic temperature $T_m(I)$.^{10,11,13,40,46} $T_m(I)$ characterizes the energy stored in the magnetic system, and gives approximate populations of the magnons $n_i \approx \frac{1}{\exp[E_i/k_B T_m] - 1}$. Here E_i are magnon energies.

We estimate the total rate of magnon generation in the macrospin approximation for F_2 . Eq. 4 gives the transverse spin absorbed by \mathbf{S} $\Delta S_z = -\Delta s_z \approx -\frac{\beta^2}{L}$. If one assumes that the longitudinal spin-transfer is associated with coherent magnon generation, the corresponding initial angle θ of classical precession of \mathbf{S} around H_{eff} would follow from $\cos(\theta) \approx 1 - \Delta s_z/L$, giving $\theta \approx \frac{\beta}{L}$. It is always larger than the estimate $\theta \approx \frac{\alpha\beta}{L}$ based on the transfer of the transverse spin (see above). This means that scattering from a coherent state of \mathbf{S} (e.g. $|L, L\rangle$) to another (tilted) coherent state constitutes only a fraction of all the scattering processes. The transfer of longitudinal spin is largest when $\alpha = 0$; then the excitation is completely incoherent, since $\Delta s_x = 0$. Incidentally, in typical current-driven switching experiments, the magnetizations M_1 and M_2 of layers F_1 and F_2 , correspondingly, are either parallel or antiparallel to each other.^{12,13,15,16,17} M_2 is related to \mathbf{S} by the gyromagnetic

ratio. Electrons flowing through F_2 then do not have a spin component perpendicular to \mathbf{S} . In this case $\alpha\beta = 0$, and the transverse spin transfer, and thus coherent excitation, vanishes.

Eq. 4 clarifies a popular misconception that the transverse electron spin component can be elastically (without electron spin-flipping) transferred to the magnetization. In this context, the probability of electron spin-flipping is identified with the longitudinal spin transfer. In the framework of the macrospin model, at large L the probability of electron spin-flip (or equivalently magnon generation) decreases as $1/L$. On the other hand, the x, y (transverse at small excitation levels) components of angular momentum, associated with excitation of uniform precession, are proportional to L (per magnon). Thus, in the large- L limit, the coherent magnon generation gives transverse spin transfer (per scattering electron) independent of L , consistent both with ST and the formalism of electron-magnon scattering. These arguments, of course, are valid only in the macrospin approximation (see below).

Because we do not consider the spatial components of the magnetic system and the electron wave function, our model does not apply to finite-wavelength magnons. We can qualitatively describe such excitations by breaking up the magnetic layer into N sufficiently small interacting elements with spins $L_i = L/N$, $i = 1..N$, in the spirit of micromagnetic models. The probability to excite one of these elements and not the others is then a rough measure of the probability to excite a magnon with wavelength of about the size of the element. According to Eq. 4, $\Delta s_z \propto 1/L$, so the probability to excite magnons with shorter wavelengths may be expected to be higher.

In the limit of small exchange stiffness of F_2 , we can replace our macrospin \mathbf{S} pointing along the z -direction, with a system of $2L$ weakly interacting electrons with spin $s_z = 1/2$. Our problem of conduction electron scattering on a macrospin can now be replaced with another, where we add one electron with a spin \mathbf{s} , and then remove one electron from the system. When the conduction electron spends a sufficiently long time in F_2 , $V_{ex} > \hbar/t$, the outgoing electron will be any one of the $2L+1$ electrons in the system, and will have spin projection $s_z = 1/2$ with a large probability $P > 1 - 1/(2L)$. The difference between this result and Eq. 4 is due to the excitation of magnons with finite wavelengths. This (grossly oversimplified) argument demonstrates again that all the magnetic modes are excited by the current, limited only by energy conservation. It can be estimated that in typical current-switching experiments at not too large applied fields, energy conservation can be satisfied for a large number of magnetic modes: typical energies and spacings between low-energy magnetic modes in transition metal magnetic nanopillars of submicron size are $\approx 10\mu\text{eV}$, while typical thermal electron energies are $\approx 25\text{ meV}$ at 295 K , the temperature at which most experiments are performed, or $\approx 0.3\text{ meV}$ at 4.2 K . Moreover, at typical experimental switching currents of several mA, the electron energies

due to the voltage applied to the sample are ≈ 1 meV, also much larger than the energies of the lowest magnetic modes.

Relating our arguments for current-driven excitation of finite-wavelength magnons to ST, we notice that the finite-wavelength magnons do not conserve the length of \mathbf{S} , thus violating the coherent approximation underlying ST: generally, $\Delta s_x = 0$ for these modes: when they are excited by the current, spin transfer transverse to the *total* magnetic moment of F_2 does not occur. Recently, local arguments in the framework of ST were made in favor of excitation of finite-wavelength magnetic modes.³⁴ Just like the original ST dealing only with the uniform precession, this model captures only the classical (i.e. in this case locally coherent) magnetic dynamics. The local spin-torque effect also requires a semiclassical approximation for the conduction electrons, in contrast to the original ST, which treats electrons quantum-mechanically.¹

We now consider a more general case of scattering with \mathbf{S} initially in $|M\rangle$, $M < L$ state. From Eq. 2,

$$\Delta s_z = \frac{1}{2(2L+1)^2} [|\beta|^2((2L+1)^2 - (2M-1)^2) - |\alpha|^2((2L+1)^2 - (2M+1)^2)]. \quad (5)$$

The first term on the right describes the probability of magnon generation by a spin-down electron, the second describes magnon absorption by a spin-up electron. An important limit of Eq. 5 is $n \ll L, M$. The magnon emission probability is then

$$P_e = \frac{|\beta|^2((2L+1)^2 - (2M-1)^2)}{2(2L+1)^2} \approx |\beta|^2 \frac{1+n}{L}, \quad (6)$$

giving both spontaneous (independent of n) and stimulated ($\propto n$) generation of magnons by the current.² The magnon absorption probability is

$$P_a = \frac{|\alpha|^2((2L+1)^2 - (2M+1)^2)}{2(2L+1)^2} \approx |\alpha|^2 \frac{n}{L}. \quad (7)$$

Eqs. 6,7 reproduce the general Einstein formulae for bosons excited by an external field, valid also for the generation of finite-wavelength magnons. Although the Einstein formulae give correct values for magnon generation rates, they do not contain information about the coherence of these excitations. ST shows that coherence is related to the transverse spin-conservation, not adequately addressed in the formalism of electron-magnon scattering.

Another important limit of Eq. 5 is $0 < M \ll L$, at high excitation level of \mathbf{S} . This limit likely corresponds to the high-field reversible switching regime in the experiments with nanopillars¹³. For $0 < M \ll L$, Eq. 5 gives

$$\Delta s_z \approx (|\beta|^2 - |\alpha|^2)/2, \quad (8)$$

expressing saturation of the magnon excitation probability. The z-component of the electron spin, which is now

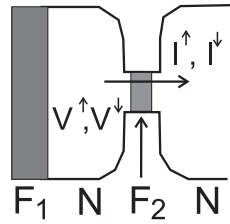


FIG. 1: Schematic of our model for the spin-dependent transport through the nanopillars, as explained in the text.

perpendicular \mathbf{S} , is completely absorbed by \mathbf{S} , in agreement with ST. However, even in this limit, the excited state of \mathbf{S} can be completely incoherent: all the projections (x, y, and z) of \mathbf{S} in the state $|L, 0\rangle$ vanish, i.e. it is a purely quantum state. Therefore, Eq. 8 represents a generalization of the ST result to the highly excited incoherent magnetization states. Below, we argue that the saturation of magnon generation is likely responsible for the behaviors associated with the reversible switching.

To summarize this section, Eq. 4 shows that ST captures only a small, coherent part of the current-driven excitations. The Einstein formulae Eqs. 6,7 describe the current-driven excitations in terms of electron-magnon scattering, but they do not provide information about the level of coherence of these excitations. We gave arguments that coherence may not be important in typical experiments. With this assumption, in Section III we use the electron-magnon scattering formalism, and effective temperature description for the magnetic excitations, to reproduce the experimental current-driven magnetization switching behaviors.

III. CURRENT-DRIVEN SWITCHING

In this Section, we show how incoherent current-driven magnetic excitations of F_2 , rather than a coherent rotation of \mathbf{S} due to the spin-torque mechanism, may lead to the experimental current-driven behaviors. To completely eliminate the coherence associated with the spin-torque effect, we assume that equilibrium orientation of the magnetization M_1 is (anti)parallel to M_2 , due to the shape anisotropy of the nanopillar F_2 .

Evolution of a system with many excited modes can be described in terms of the density matrix dynamics. Besides analytical and computational difficulties, such a description would involve a large number of presently unknown parameters. Instead, we now show how an approximate effective temperature description of the magnetic system excited by current, and current-driven magnon generation rates given by Eqs. 6,7, reproduces typical current-driven switching experiments with nanopillars.^{12,13,15,16,17} This analysis does not prove that the current-driven excitations are thermalized. Rather, it shows that coherence of the excitations is not essential in these experiments.

Fig. 1 illustrates our quasi-ballistic model of transport through a $F_1/N/F_2$ trilayer, similar to the circuit model of Brataas *et al.*⁴¹ The nanopillar F_2 is represented by a high-resistivity constriction, separating low-resistivity reservoirs. If we neglect inelastic scattering in F_2 (including spin-flipping), and separately consider two different spin channels, this system can be treated in the Landauer formalism. To account for two separate spin channels, one can formally replace each reservoir in Fig. 1 with two completely spin-polarized reservoirs. The electron spin-flipping can then be treated as transmission between spin-up and spin-down reservoirs.

We model the spin-polarizing effect of the large ferromagnet F_1 by different spin-up and spin down potentials in the left reservoir, V^\uparrow and V^\downarrow . The spin states are defined with respect to the majority spin orientation in F_2 (i.e. opposite of the magnetization M_2). We take $V = 0$ in the right reservoir, i.e. neglect the spin accumulation there. I^\uparrow , I^\downarrow are spin-up and spin-down currents through the constriction. Positive I is from F_1 to F_2 . We define ΔV , p by $\Delta V = V^\uparrow - V^\downarrow = 2pV$. Here $V \approx (V^\uparrow + V^\downarrow)/2$ is related to the voltage across the sample. If F_2 is removed, p becomes the current polarization in the constriction. Spin-dependent scattering at each of the interfaces of F_2 is described by conductances $G^\uparrow = 2I^\uparrow/V^\uparrow$, $G^\downarrow = 2I^\downarrow/V^\downarrow$.⁴¹ We introduce an additional ballast resistance R_0 in both spin channels, giving a correction to these expressions. R_0 accounts for contributions from F_1 , and other bulk and contact resistances. It controls the asymmetry of the switching currents in the opposite directions. We neglect multiple scattering, so the interface resistances add.

At small H , the current-driven switching occurs through thermal activation at relatively low magnetic excitation levels, with magnon generation rates approximately described by Eqs. 6,7.^{6,13} A diffusive model for the stimulated current-driven magnon emission, driven by spin-accumulation, was developed in Ref. 2, where the energy was used as the only parameter characterizing the electron distributions. The ballistic model of Fig. 1 needs to incorporate the nonequilibrium distributions in momentum space, and hot electron transport through the constriction. However, such extensions of Ref. 2 would have limited physical meaning, since the semiclassical approximation, involved in the distribution function formalism, breaks down on the relevant length scales of the constriction.

Instead, we use ballistic scattering theory arguments to obtain an expression for the spin-flip scattering rates in the constriction. For simplicity we neglect magnon energies, which (for the low-energy modes) are smaller than the typical conduction electron energies at the bias voltages leading to switching, and consider spin-flipping of electrons both transmitted and reflected at the interfaces. To avoid complications associated with scattering among different spin-channels, we separately consider spontaneous and stimulated magnon emission.

First, we assume $p = 0$, i.e. the current from F_1 is un-

polarized. In this limiting case, the spin-flip scattering back into the same reservoir is suppressed. Both spin-up and spin-down electrons experience spin-flip scattering with identical matrix elements, as follows from the unitarity of the scattering matrix. Because of the spontaneous emission (see Eq. 6), the total rate of magnon generation by the spin-down electrons is higher than the magnon absorption rate by the spin-up electrons, and is proportional to the number of electrons transmitted by F_2 , $\Gamma_{sp} \approx A|eV|$. Here A is a constant determined by the parameters of the constriction and the electron-magnon scattering matrix element, $e = -|e|$ is the electron charge, and the number of transmitted electrons is proportional to the voltage drop across the constriction (Ohms law). The spin-polarization due to F_2 is usually small because of the ballast resistance R_0 , so we do not consider its effect on the spontaneous magnon generation.

We now consider the effect of finite polarization $p \neq 0$ in the left reservoir (Fig. 1), essential for stimulated magnon generation. For simplicity, we assume here that every electron spin-flipping is associated with magnon emission or absorption. The spin-flipping due to spin-orbit interaction does not qualitatively change our arguments. The number of open spin-flip channels for transmission from spin-down states in the left reservoir to spin-up states in the right reservoir is proportional to V^\downarrow , therefore the corresponding stimulated magnon emission rate in F_2 is $\Gamma_{em} \approx B_1 e k_B T_m V^\downarrow$, with a constant B_1 . In terms of Landauer-Buttiker formalism, $B_1 e k_B T_m$ is related to the coefficient of transmission from the spin-down to the spin-up channels. We use $n_i \approx k_B T_m/E_i$ for degenerate magnon populations. We note that in the effective temperature terminology, magnon emission leads to magnetic heating, while magnon absorption leads to current-driven magnetic cooling. By a similar argument, $\Gamma_{ab} \approx B_1 e k_B T_m V^\uparrow$ is the stimulated magnon absorption rate, due to spin-up electrons in the left reservoir transmitted into the right reservoir with a spin-flip. In the remaining spin-flip scattering processes, the spin-up (spin-down) electrons in the left reservoir are reflected back into the same reservoir, with a spin-flip. The rate for these processes is $B_2 e k_B T_m (V^\downarrow - V^\uparrow)$. The total stimulated magnon generation rate is then $\Gamma_{st} \approx B e k_B T_m (V^\downarrow - V^\uparrow) = -2B e p V k_B T_m$, where $B = B_1 + B_2$.

In the relaxation time approximation, the spin-lattice relaxation rate is $\Gamma_{ph} \approx \gamma k_B (T_m - T_{ph})$, where γ is related to the Gilbert damping parameter in the classical dynamic equations.² In thin films, damping is expected to have a large contribution from electron-magnon scattering.⁴² In the magnetic system with a nonequilibrium electron distribution, damping then becomes dependent on the current amplitude and polarization. We neglect this dependence here. In a steady state, $\Gamma_{st} + \Gamma_{sp} = \Gamma_{ph}$, giving

$$k_B T_m \approx \frac{|eV|A/\gamma + k_B T_{ph}}{1 + 2peVB/\gamma}. \quad (9)$$

We use Eq. 9 to describe current-driven thermally acti-

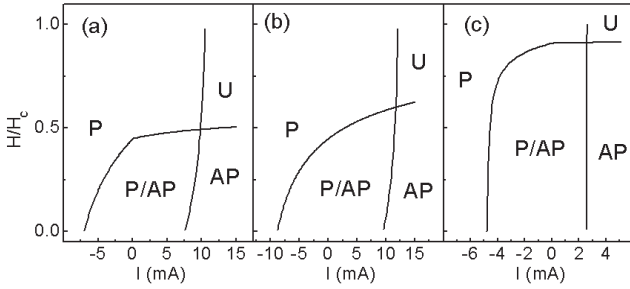


FIG. 2: Calculated magnetization stability diagrams: (a) for Co/Cu/Co nanopillars at 295 K, $A/\gamma = 2$, $B/\gamma = 0.1 \text{ meV}^{-1}$, (b) same as (a), but with $A = 0$, (c) for Py/Cu/Py nanopillars at 4.2 K, $A/\gamma = 0.1$, $B/\gamma = 0.3 \text{ meV}^{-1}$. (AP)P denotes a region where (anti)parallel configuration of the magnetic layers is stable, P/AP is a bistable region. Both orientations are unstable in U.

vated switching over a magnetic barrier U , given by the shape anisotropy of the nanopillar. The switching occurs at $k_B T_m \approx \frac{U(H, T_m)}{\ln(t_{exp}\Omega)} \approx \frac{U}{16}$, for a data acquisition time t_{exp} of 1 second per point, and an effective attempt rate $\Omega \approx 10^7 \text{ s}^{-1}$.⁴³ When thermal activation is included in ST, the effect of I is equivalent to renormalization of U .³³ This can also be formally rewritten as renormalization of T_{ph} ,⁸ giving an expression similar to Eq. 9, but without the spontaneous term. This similarity is superficial, since ST result is based on a completely different, coherent picture of the current-driven magnetic dynamics.

We use an approximation $U(H, T_m) \approx U_0 \sqrt{1 - T_m/T_c} (1 \mp H/H_c)^2$.^{13,33} Here the sign depends on the mutual orientations of H and M_2 , T_c is the Curie temperature of F_2 , and H_c is determined by the shape anisotropy of the nanopillar. For a given value of H , we solve the equation $U(H, T_m) = 16k_B T_m$ for T_m , to obtain the effective temperature $T_0(H)$ at which the switching occurs. Taking into account the relationships between the currents and voltages $V^{\uparrow(\downarrow)} = I^{\uparrow(\downarrow)}(R_0 + 2/G^{\uparrow(\downarrow)})$, from Eq. 9 we find the switching current

$$I_s = -\frac{k_B(T_0(H) - T_{ph})(\frac{1+p}{R_0 + \frac{G^{\downarrow}}{G^{\uparrow}}} + \frac{1-p}{R_0 + \frac{G^{\uparrow}}{G^{\downarrow}}})}{\text{sign}(p)eA/\gamma + 2epk_B T_0(H)B/\gamma} \quad (10)$$

For Co/Cu/Co or Py/Cu/Py (Py is typically Ni₈₀Fe₂₀) nanopillars with areas $\approx 10^{-14} \text{ m}^2$, we use $G^{\uparrow} = 30 \text{ S}$, $G^{\downarrow} = 6 \text{ S}$, $p = \pm 0.6$,⁴⁴ with the sign given by the mutual orientations of the magnetic layers. To compare with the published data,^{6,12,13,16} we use $T_c = 1400 \text{ K}$ and $U_0 \approx 1.5 \text{ eV}$ for 2.5 nm thick Co nanopillars with typical dimensions of $140 \times 70 \text{ nm}$, $T_c = 800 \text{ K}$ and $U_0 \approx 0.7 \text{ eV}$ for 6 nm thick Py nanopillars with similar dimensions. Fig. 2(a) shows a magnetization stability diagram obtained from Eq. 10 for Co/Cu/Co nanopillars at $T_{ph} = 295 \text{ K}$. $A/\gamma = 2$, $B/\gamma = 0.1 \text{ meV}^{-1}$, $R_0 \approx 1 \Omega$ give a good overall agreement with the published data. Microscopic evaluation of A , B is outside

the scope of this work. Within our model, A and B are determined by the same electron-magnon scattering matrix elements. The stimulated scattering rates are proportional to $k_B T_m B = B n_i / E_i$, while the spontaneous emission rate is simply proportional to A with a similar pre-factor. Thus, $A/B \approx 20 \text{ meV}$ is a crude measure of the typical energies E_i of magnons excited by the current. Even assuming that this is an overestimate, Eqs. 9,10 may be altered if the high magnon energies are taken into account when electron-magnon scattering is considered. The corresponding magnon wavelength is $\approx 1 \text{ nm}$, supporting our estimates that the current excites predominantly short-wavelength magnons.

For qualitative comparison with ST,^{8,33} Fig. 2(b) shows the same calculation as in Fig. 2(a), but without the spontaneous term. The main difference is the lack of a knee in the stability line at $I = 0$, evident in some published data.^{6,12} A knee at $I < 0$ in some ST-based calculations^{6,17} is different, it is due to a singularity associated only with the $T_{ph} = 0$ limit. The knee in Fig. 2(a) is due to the contribution of the spontaneous emission in Eq. 9. A competition between the stimulated magnetic cooling and spontaneous heating at $I > 0$ in the state with antiparallel magnetizations gives overall weak cooling. In some cases,⁴⁵ the switching fields decrease both at $I > 0$ and $I < 0$, indicating that heating occurs instead of cooling. Spontaneous magnon emission may also be responsible for some of the current-driven phenomena in single magnetic layers.^{3,10,19,45} As our ballistic analysis shows, the stimulated magnon emission vanishes in this case ($p = 0$).

We were able to model the published 295 K Py/Cu/Py data with A, B values similar to those used for Co. Fig. 2(c) shows a calculation for Py/Cu/Py at $T_{ph} = 4.2 \text{ K}$. It reproduces the nearly "square" switching diagram.¹³ $A/\gamma = 0.1$, $B/\gamma = 0.3 \text{ meV}^{-1}$, give good overall agreement with the experiment. The differences with the 295 K values reflect a decrease of the average energy of magnons excited by I . The dependence of A, B on T_{ph} does not appear in our model, and warrants a more detailed analysis of the temperature dependence of electron-magnon scattering.

Beyond the switching diagrams, we identify the threshold I_t for a large increase of T_m in the state with parallel magnetizations of F_1 , F_2 at $I > 0$,¹³ with the divergence of Eq. 9 at $-eV \rightarrow \gamma/(2pB)$. As we showed above, magnon generation saturates at large magnetic excitation amplitude, becoming nearly independent of T_m . Eq. 9 is then replaced by a linear relation $T_m \approx T_{ph} + KpV$, where K is a constant determined by the magnetic relaxation rate. A similar (with a different constant term) linear relation has been empirically proposed to explain the lack of temperature dependence of telegraph noise dwell times variations with current.¹³ In contrast, a formal relation $T_m \propto T_{ph}$ expected for the ST³³ does not fit those data.

IV. SUMMARY

In Section II, we demonstrated that spin-polarized current flowing through a ferromagnet leads to both coherent and incoherent magnetic excitations (not conserving the expectation value of the magnetic moment). Only the coherent excitations are captured by the spin-torque model (ST). On the other hand, the electron-magnon scattering framework describes all the excitations, but does not give information about the level of excitation coherence. We argue that coherence of excitations may not be significant or important in typical current-switching experiments, due to direct generation of incoherent excitations by the current, and nonlinear magnetic interactions.

In Section III, we describe an incoherent excitation of F_2 in terms of a current-dependent magnetic temperature, and show that this approximation is consistent with the results of typical current-switching experiments. Without the spontaneous magnon generation term, Eq. 9, describing the effect of current on the magnetization, is mathematically similar to the finite temperature result of ST. The two models, however, are based on completely different underlying physical pictures. Here we give two examples which distinguish these models. First, the spontaneous magnon generation term in Eq. 9 is absent in ST. It gives: i) excitations at small T_{ph} for layers with parallel static magnetizations, a nominal configuration in typical current-switching ex-

periments; ii) current-driven excitations by unpolarized current,^{3,10,19,45} iii) a knee in the magnetization stability curve at $I = 0$,^{12,47} related to stronger current-driven magnetic heating than the cooling achieved by reversal of the current. Second, Eq. 9 suggests that the current-driven excitation rate may be enhanced by increasing the polarization¹⁴ and electron-magnon scattering rates. Larger excitation levels give smaller switching currents, needed for possible technological applications of direct current-driven switching in magnetic memory devices. Higher scattering rates may be achieved by decreasing the effective magnetic volume excited by the current (value of L in Eq. 6), through interface roughness, alloying, or building complex magnetic layers with a small exchange strength at the interfaces. The enhancement of electron-magnon scattering at rough interfaces, and in magnetically disordered alloys, can be understood not only in terms of the oversimplified model of Section II, but also from a more rigorous calculation of electron-magnon scattering amplitudes.⁴⁶ In contrast, ST gives reduced transverse spin transfer for smaller magnetic volume ($\propto L$ in Eq. 4), and independent of the interface roughness and magnetic disorder.

The author acknowledges helpful discussions with V.I. Kozub, N. Sinitzyn, Ya. Bazaliy, J. Bass, N.O. Birge, W.P. Pratt Jr., A.H. MacDonald, D.C. Ralph, A. Fert, support from the MSU CFMR, CSM, the NSF through Grants DMR 02-02476, 98-09688, and 00-98803, and Seagate Technology.

¹ J. Slonczewski, *J. Magn. Magn. Mater.* **159**, L1 (1996).
² L. Berger, *Phys. Rev. B* **54**, 9353 (1996).
³ E.B. Myers, D.C. Ralph, J.A. Katine, R.N. Louie, R.A. Buhrman, *Science* **285**, 867 (1999).
⁴ M. Tsai, A.G.M. Jansen, J. Bass, W.C. Chiang, M. Seck, V. Tsai, and P. Wyder, *Phys. Rev. Lett.* **80**, 4281 (1998); **81**, 493(E) (1998).
⁵ C. Heide, P. E. Zilberman, and R. J. Elliott, *Phys. Rev. B* **63**, 064424 (2001).
⁶ E. B. Myers, F.J. Albert, J.C. Sankey, E. Bonet, R.A. Buhrman, and D.C. Ralph, *Phys. Rev. Lett.* **89**, 196801 (2002).
⁷ F. J. Albert, N.C. Emley, E.B. Myers, D.C. Ralph, and R.A. Buhrman, *Phys. Rev. Lett.* **89**, 226802 (2002).
⁸ R.H. Koch, J.A. Katine, and J.Z. Sun, preprint.
⁹ M. Tsai, V. Tsai, J. Bass, A.G.M. Jansen, and P. Wyder, *Phys. Rev. Lett.* **89**, 246803 (2002).
¹⁰ J. E. Wegrowe, H. Hoffer, Ph. Guittienne, A. Fabian, L. Gravier, T. Wade, and J. P. Ansermet, *J. Appl. Phys.* **91**, 6806 (2002).
¹¹ J.E. Wegrowe, cond-mat/0306103(2003).
¹² S. Urazhdin, H. Kurt, W.P. Pratt Jr., and J. Bass, *Appl. Phys. Lett.* **83**, 114 (2003).
¹³ S. Urazhdin, N.O. Birge, W.P. Pratt Jr., and J. Bass, *Phys. Rev. Lett.* **91**, 146803 (2003).
¹⁴ S. Urazhdin, N.O. Birge, W.P. Pratt Jr., and J. Bass, cond-mat/0309191 (2003).
¹⁵ J.A. Katine, F.J. Albert, R.A. Buhrman, E.B. Myers and D.C. Ralph, *Phys. Rev. Lett.* **84**, 3149 (2000).
¹⁶ F.J. Albert, J.A. Katine, R.A. Buhrman, and D.C. Ralph, *Appl. Phys. Lett.* **77**, 3809 (2000).
¹⁷ J. Grollier, V. Cros, A. Hamzic, J.M. George, H. Jaffres, A. Fert, G. Faini, J.B. Youssef, and H. Legall, *Appl. Phys. Lett.* **78**, 3663 (2001); *ibid*, *Phys. Rev. B* **67**, 174402 (2003).
¹⁸ J. Z. Sun, D.J. Monsma, T.S. Kuan, M.J. Rooks, D.W. Abraham, B. Oezilimaz, A.D. Kent, and R.H. Koch, *J. Appl. Phys.* **93**, 6859 (2003).
¹⁹ Y. Ji, C.L. Chien, and M.D. Stiles, *Phys. Rev. Lett.* **90**, 106601 (2003).
²⁰ S.I. Kiselev, J.C. Sankey, I.N. Krivorotov, N.C. Emley, R.J. Schoelkopf, R.A. Buhrman, D.C. Ralph, *Nature* **425**, 380 (2003).
²¹ B. Oezilimaz, A.D. Kent, D. Monsma, J.Z. Sun, M.J. Rooks, and R.H. Koch, *Phys. Rev. Lett.* **91**, 067203 (2003).
²² Y.B. Bazaliy, B.A. Jones, S.C. Zhang, *Phys. Rev. B* **57**, R3213 (1998).
²³ J. Slonczewski, *J. Magn. Magn. Mater.* **195**, L261 (1999).
²⁴ X. Waantal, E.B. Myers, P.W. Brouwer, and D.C. Ralph, *Phys. Rev. B* **62**, 12317 (2000).
²⁵ J. Z. Sun, *Phys. Rev. B* **62**, 570 (2000).
²⁶ J. Slonczewski, *J. Magn. Magn. Mater.* **247**, 324 (2002).
²⁷ M. D. Stiles and A. Zangwill, *J. Appl. Phys.* **247**, 324 (2002).
²⁸ M. D. Stiles and A. Zangwill, *Phys. Rev. B* **66**, 014407 (2002).

²⁹ A. Kovalev, A. Brataas, and G. E. W. Bauer, Phys. Rev. **B 66**, 224424 (2002).

³⁰ K. Xia, P.J. Kelly, G.E.W. Bauer, A. Brataas, and I. Turek, Phys. Rev. **B 65**, 220401 (2002).

³¹ S. Zhang, P. M. Levy, A. Fert, Phys. Rev. Lett. **88**, 236601 (2002).

³² A. Shapiro, P. M. Levy, S. Zhang, Phys. Rev. **B 67**, 104430 (2003).

³³ Z. Li and S. Zhang, cond-mat/0302339.

³⁴ M.L. Polianski and P.W. Brouwer, cond-mat/0304069.

³⁵ M. Sparks, *Ferromagnetic-Relaxation Theory*, McGraw-Hill, New York, 1964.

³⁶ T. Holstein and H. Primakoff, Phys. Rev. **58**, 1098 (1940).

³⁷ H.J. Suhl, J. Phys. Chem. Solids **1**, 209 (1957).

³⁸ R.D. McMichael, D.J. Twisselmann, and A. Kunz, Phys. Rev. Lett. **90**, 227601 (2003).

⁴⁶ S.J.C.H. Theeuwen, J. Caro, K.P. Wellock, S. Radelaar, C.H. Marrows, B.J. Hickey, and V.I. Kozub, Appl. Phys. Lett. **75**, 3677 (1999).

⁴⁰ J. Hohfeld, E. Matthias, R. Knorren, and K.H. Benne-
mann, Phys. Rev. Lett. **78**, 4861 (1997).

⁴¹ A. Brataas, Yu.V. Nazarov, and G.E.W. Bauer, Phys. Rev. Lett. **84**, 2481 (2000).

⁴² Y. Tserkovnyak, A. Brataas, G.E.W. Bauer, Phys. Rev. Lett. **88**, 117601 (2002).

⁴³ R. H. Koch, G. Grinstein, G.A. Keefe, Yu Lu, P.L. Trouil-
loud, W.J. Gallagher, and S.S.P. Parkin, Phys. Rev. Lett. **84**, 5419 (2000).

⁴⁴ W. P. Pratt Jr., S.D. Steenwyk, S.Y. Chiang, A.C. Scae-
fer, R. Loloe, and J. Bass, IEEE Trans. Magn. **33**, 3505 (1997).

⁴⁵ S. Urazhdin, N.O. Birge, W.P. Pratt Jr., and J. Bass, un-
published.

⁴⁶ V.I. Kozub, private communications.

⁴⁷ S. Urazhdin, N.O. Birge, W.P. Pratt Jr., and J. Bass, cond-mat/0310472.